Electronic Supplementary Material (ESI) for Environmental Science: Nano.
This journal is © The Royal Society of Chemistry 2021

Supporting Information

Oxygen Vacancy Modulated Interface Chemistry: Identifying Iron(IV) in Heterogeneous Fenton Reaction

Yaqin Yu[†,‡], *Haoze Chen*[†,‡], *Li Yan*[†], *Chuanyong Jing*[†,‡,*]

[†] State Key Laboratory of Environmental Chemistry and Ecotoxicology, Research Center for Eco-Environmental Sciences, Chinese Academy of Sciences, Beijing 100085, China.

[‡] University of Chinese Academy of Sciences, Beijing 100049, China.

Tel: +86 10 6284 9523; Fax: +86 10 6284 9523

*E-mail: cyjing@rcees.ac.cn

***Corresponding author:** Dr. Chuanyong Jing

1. Chemicals and materials.

Methyl phenyl sulfoxide (MPSO), methyl phenyl sulfone ($MPSO_2$), 5,5-dimethyl-1-pyrrolin-N-oxide (DMPO), tert-butanol (TBA), *p*-benzoquinone (*p*-BQ), and dimethyl sulfoxide (DMSO) were purchased from Sigma Chemical (USA). WCl_6 and $FeCl_2$ were obtained from J&K Scientific LTD (China). Methyl orange (MO), H_2O_2, $FeCl_3 \cdot 6H_2O$, and ethanol were purchased from Sinopharm Chemical Reagent (China). All reagents were analytical grade and used directly without further purification.

$WO_{2.72}$ was synthesized by a traditional hydrothermal method.[1] Typically, 0.5 g of WCl_6 was dissolved in 50 ml ethanol, and the mixed solution was transferred into a 100 ml Teflon-lined autoclave. The hydrothermal reaction was conducted at 180℃ for 12 h. After cooling, the as-obtained precipitates were washed by ethanol and dried at 60℃ in a vacuum oven. The Vo-rich WO_{3-x} samples with different Vo contents were obtained by calcining $WO_{2.72}$ in a 15% H_2 atmosphere at 200, 300, and 400℃ for 2 h. The Vo-poor WO_{3-x} was prepared by annealing $WO_{2.72}$ in an O_2 atmosphere at 200℃ for 2 h.

2. Characterization.

The morphology of WO_{3-x} was characterized using field emission scanning electron microscopy (FE-SEM, SU-8000, Hitachi, JPN) and high resolution-transmission electron microscopy (HRTEM, JEM-2100F, JEOL. Ltd., JPN). X-ray photoelectron spectra (XPS) were analyzed with Al Kα X-ray radiation at 1486.8 eV (AXIS SUPRA, SHIMADZU, JPN). The electron paramagnetic resonance (EPR) signals were recorded on a Bruker EMX plus spectrometer (LOT-Oriel Gmbh&Co. KG, Germany). Raman spectra were collected on a laser confocal microscopy Raman spectrometer (LabRAM HR Evolution, HORIBA, JPN) with excitation wavelength at 532 nm.

In-situ X-ray absorption near-edge spectroscopy (XANES) was performed on beamline 01C1 at the National Synchrotron Radiation Research Center (NSRRC) in Taiwan, China. The XANES spectra of Fe K-edge (7,112 eV) and W L_3-edge (10,207 eV) were collected to characterize the electron transfer between Fe and WO_{3-x}. The O K-edge spectra (543.1 eV) were collected to probe the change of unoccupied electronic states of WO_{3-x} with different Vo contents.

3. Elimination of pollutants in Vo-dependent Fenton system.

The performance of Vo-dependent Fenton was evaluated using methyl orange (MO) as a typical contaminant. Specifically, 50 mg WO_{3-x} was dispersed in 50 mL 20 mg/L MO solution (pH=5) with 0.34 mmol/L Fe^{II}. After stirring in dark for 30 s, 0.5 mmol/L H_2O_2 was added to the suspension. The suspension was magnetically stirred in the dark. 1 mL aliquots were collected and filtered through a 0.22 μm membrane filter. The concentration of MO was analyzed using a spectrophotometer (Varioskan Flash, Thermo, US).

4. *In-situ* FTIR measurements.

Flow-cell Fourier transform infrared (FTIR) experiments were performed using a Thermo-Nicolet iS50R FTIR spectrometer. The catalyst film was deposited on the ZnSe ATR crystal with a 2.0 g/L $WO_{2.72}$ suspension. The Fe^{II} and H_2O_2 solutions were pumped with a flow rate of 0.3 ml/min, and the reaction spectra were monitored with 256 scans at 4 cm^{-1} resolution. After baseline correction for the IR spectra, two-dimensional correlation spectroscopy (2D-COS) analysis was carried out using 2Dshige software (Shigeaki Morita, Japan). The signs of the synchronous correlation peaks Φ (v_1, v_2) and asynchronous correlation peaks Ψ (v_1, v_2) reveal the sequential order of intensity change of IR bands. Briefly, the change in the spectral intensity at band v_1 occurs prior to that at v_2 if Φ (v_1, v_2) and Ψ (v_1, v_2) have the same signs, while the order is reversed if Φ (v_1, v_2) and Ψ (v_1, v_2) have opposite signs. The changes at v_1 and v_2 occur simultaneously if Ψ (v_1, v_2) is zero. The peak fittings of IR spectra were performed with Peakfit v.4.12 software using the second derivative fitting algorithm.

5. Detection of ROS and Fe species.

To investigate the role of ROS in the Vo-dependent Fenton system, trapping experiments were conducted by adding radical scavengers. To evaluate the conversion efficiency of Fe^{III} to Fe^{II}, 1.0 g/L $WO_{2.72}$ was added into an 0.14 mmol/L Fe^{III} solution. The produced Fe^{II} was detected with 1,10-phenanthroline monohydrate as the color-developing agent. The generation of Fe^{IV} was evaluated by measuring the concentration of MPSO and $MPSO_2$ with high-performance liquid chromatography (HPLC, Shimadzu LC 20A) equipped with a diode array detector (271 nm). Chromatographic separations were conducted using a C18 LC column. Isocratic elution was carried out with 95% water containing 0.1% formic acid and 5% methanol containing 0.1% formic

acid at a flow rate of 0.4 mL/min. The dissolved Fe^{IV} and surface Fe^{IV} were respectively determined. To determine the dissolved Fe^{IV}, the samples were collected and filtered through a 0.22 μm filter. 1mL of the filtrates was immediately mixed with 1 mmol/L MPSO and 10 mmol/L TBA solution. The purpose of the addition of MPSO was to react with dissolved Fe^{IV}, and TBA solution was added to avoid the interference of $^{\bullet}OH$ radical in MPSO oxidation. The concentration of the total Fe^{IV}, including dissolved and surface Fe^{IV}, was measured by the same steps as that of dissolved Fe^{IV} except for the addition of MPSO before filtration. The surface Fe^{IV} concentration could be calculated by subtracting the dissolved Fe^{IV} from the total Fe^{IV} concentration.

6. DFT calculations.

Spin-polarized density functional theory (DFT) calculations were performed with the VASP 5.4 package. The exchange-correlation energy was calculated with the Perdew-Burke-Ernzerhof (PBE) of generalized gradient approximation (GGA) method.[2] The periodic valence electron wavefunctions were expanded in plane-wave basis sets with an energy cut-off of 400 eV. $WO_{2.72}$ {010} facet was cleaved from the optimized bulk structures with four-layer thickness. The vacuum gap was set as 20 Å to eliminate the interaction between periodic images along the perpendicular axis. Only one Gamma K-point is sufficient to describe the slabs with large lattice parameters (more than 15 Å) and considerable atoms in a unit cell (more than 150 atoms). The extended versions of pseudopotential basis sets as W_sv and Fe_pv in accord with the PBE calculation were used to describe the tungsten and iron in series of models. The bottom of the slab was saturated with ten pseudo hydrogen atoms with a formal charge of 1.0 and eight pseudo hydrogen atoms with a formal charge of 1.25 to improve the convergence of the interaction electronic energy calculation. An on-site Coulomb potential (DFT+U) correction was applied to the 5*d* electron of W atoms with U=6.2 eV.[3]

In terms of the pure facet of $WO_{2.72}$ {010} and the series of configurations with iron complex adsorption, the top two layers of the slabs were allowed to relax and the convergence threshold for structural optimization was set to be 10^{-5} eV for the energy calculation and 0.05 eV $Å^{-1}$ for the force calculation. Two types of iron complexes were described as follows. The initial Fe^{II} complex with high spin (four up electrons) was placed upon the facet through interaction with the bridge oxygen across the site of an

oxygen vacancy. The final product was a Fe^{IV} complex with high spin (four up electrons) accompanied by a proton transfer to the bridge O atom and -OH bound with an unsaturated W atom. The reaction energy of the Fe^{IV} formation process can be written as the following equation

$$E_{reaction} = E(\equiv OFe^{IV}O) + E(H_2O) - E(\equiv OFe^{II}) - E(H_2O_2)$$

The calculated electronic energies of the species are shown in **Table S1**.

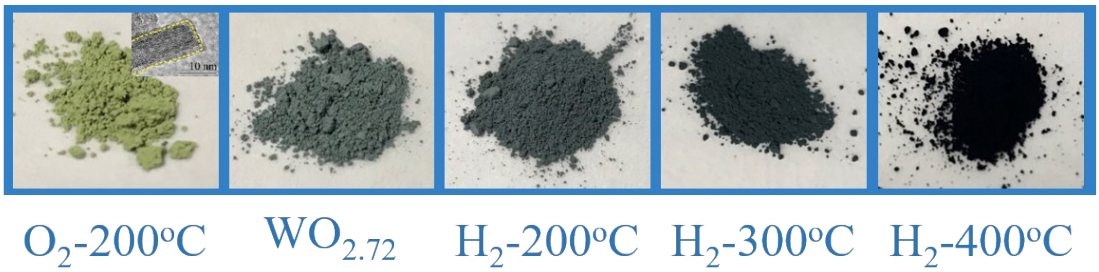

Figure S1 Color of $WO_{2.72}$ treated with O_2 at 200°C, and H_2 at 200°C, 300°C, 400°C. Inset shows the HRTEM image of $WO_{2.72}$ treated with O_2 at 200°C for 2 h.

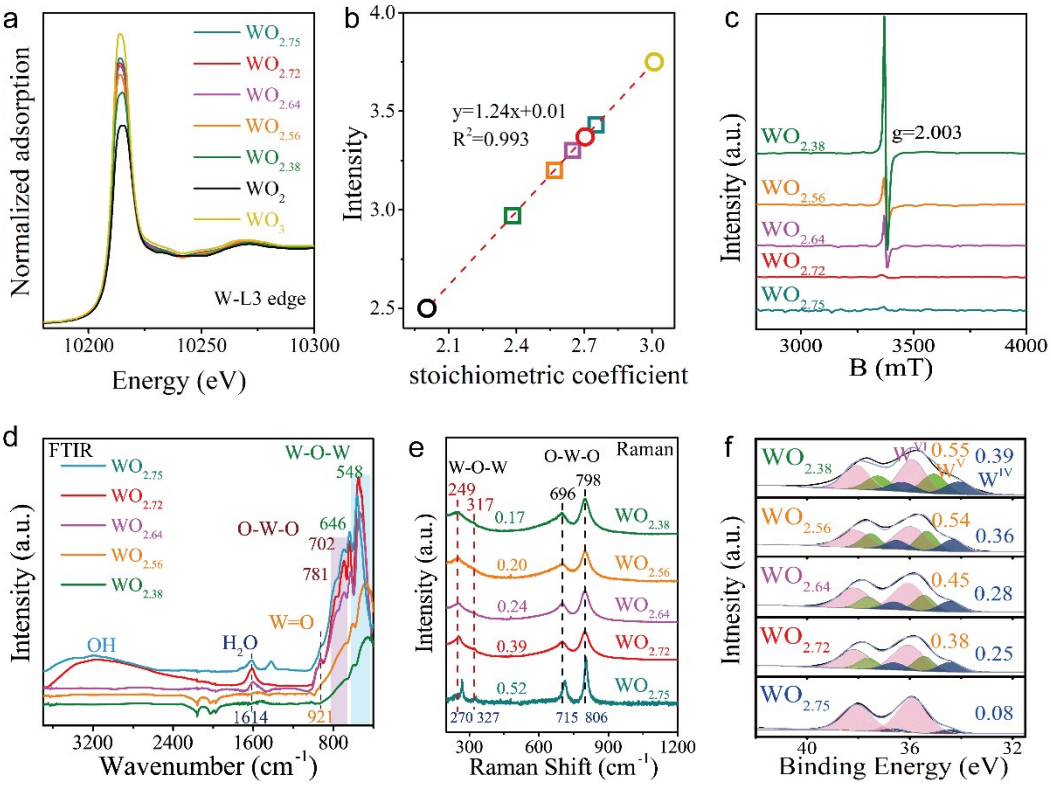

Figure S2 (a) W L_3-edge spectra of WO_2, WO_3, $WO_{2.75}$, $WO_{2.72}$, $WO_{2.64}$, $WO_{2.56}$, and $WO_{2.38}$. (b) A linear relationship between the intensity of the W L_3-edge white-line peak and stoichiometric coefficients (3-x) of WO_{3-x}. (c) Low-temperature EPR spectra of $WO_{2.75}$, $WO_{2.72}$, $WO_{2.64}$, $WO_{2.56}$, and $WO_{2.38}$. (d) FTIR, (e) Raman, and (f) high-resolution W 4f XPS spectra of $WO_{2.75}$, $WO_{2.72}$, $WO_{2.64}$, $WO_{2.56}$, and $WO_{2.38}$.

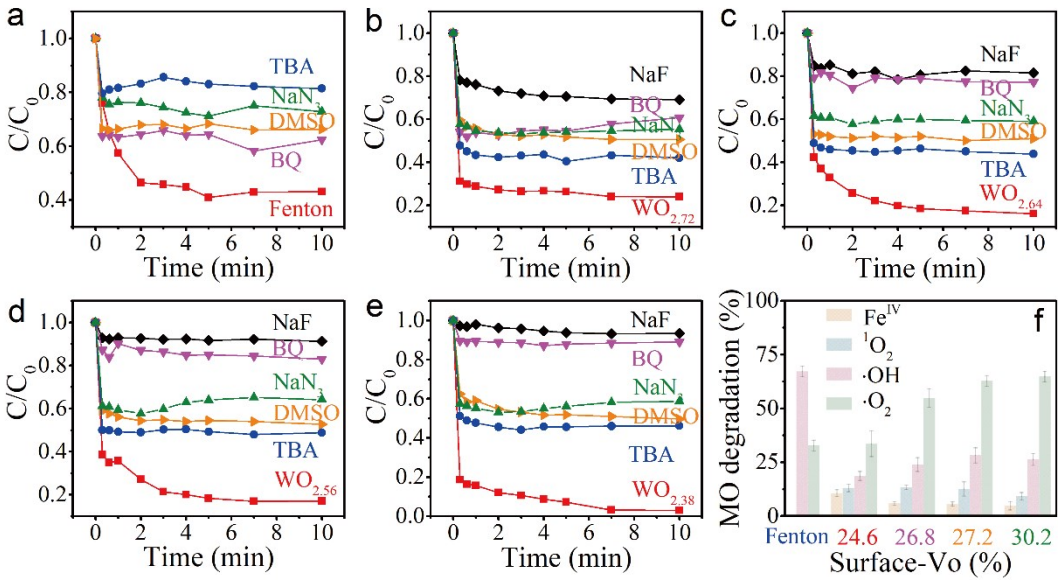

Figure S3 Removal of MO dyes over (a) Fenton, (b) $WO_{2.72}$, (c) $WO_{2.64}$, (d) $WO_{2.56}$, and (e) $WO_{2.38}$ co-catalysts in the presence of different scavengers. (f) MO degradation percentage after adding various ROS scavengers as function of the surface-Vo percentage. Experimental conditions: [MO] = 20 mg/L, [Fe^{II}] = 0.34 mmol/L, [H_2O_2] = 0.5 mmol/L, [WO_{3-x}] = 1.0 g/L. BQ was added for quenching $^{\bullet}O_2^-$, TBA for $^{\bullet}OH$, DMSO for both Fe^{IV} and $^{\bullet}OH$, and NaN_3 for both $^1O_2$ and $^{\bullet}OH$.

The formation of Fe^{IV} was evidenced by the use of its specific probe molecule, where MPSO was oxidized to $MPSO_2$ through an oxygen atom transfer. The dissolved Fe^{IV} and surface Fe^{IV} were respectively determined. To determine the dissolved Fe^{IV}, the samples were collected and filtered through a 0.22 μm filter. 1mL of the filtrates was immediately mixed with 1 mmol/L MPSO and 10 mmol/L TBA solution. The purpose of the addition of MPSO was to react with dissolved Fe^{IV}, and TBA solution was added to avoid the interference of $^{\bullet}OH$ radical for MPSO oxidation. As shown in **Figure S4a**, MPSO was not oxidized to $MPSO_2$ by dissolved Fe^{IV}. The concentration of total Fe^{IV}, including dissolved and surface Fe^{IV}, was measured by the same steps as that of dissolved Fe^{IV} except for the addition of MPSO before filtration. The surface Fe^{IV} concentration could be calculated by subtracting the dissolved Fe^{IV} from the total Fe^{IV} concentration. As shown in **Figure S4b**, the concentration of MPSO decreased from 0.94 to 0.85 mmol/L and $MPSO_2$ increased from 0.01 to 0.08 mmol/L, suggesting

the presence of Fe^{IV} in the WO_{3-x}+Fe^{II}+H_2O_2 system. Then, MPSO was oxidized to $MPSO_2$ by surface Fe^{IV} in the WO_{3-x} co-catalytic Fenton system.

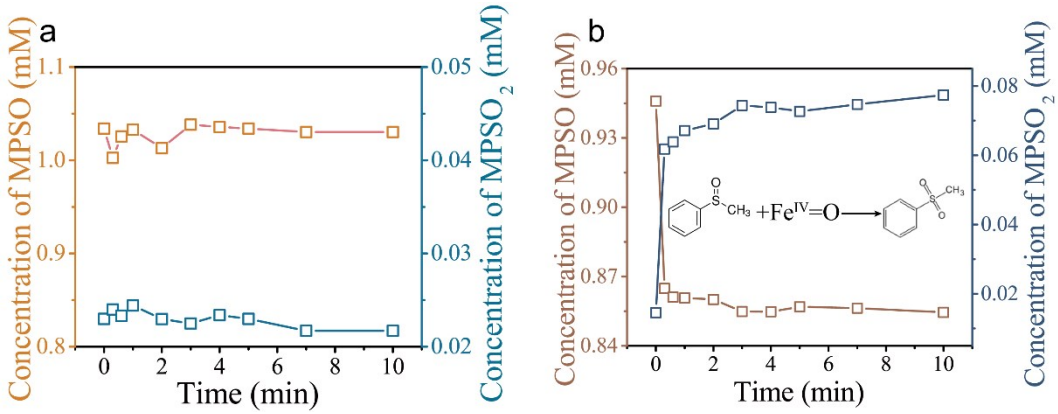

Figure S4 (a) MPSO reacted with dissolved Fe^{IV} in $WO_{2.72}$ co-catalytic Fenton system. (b) MPSO reacted with total Fe^{IV} in $WO_{2.72}$ co-catalytic Fenton system.

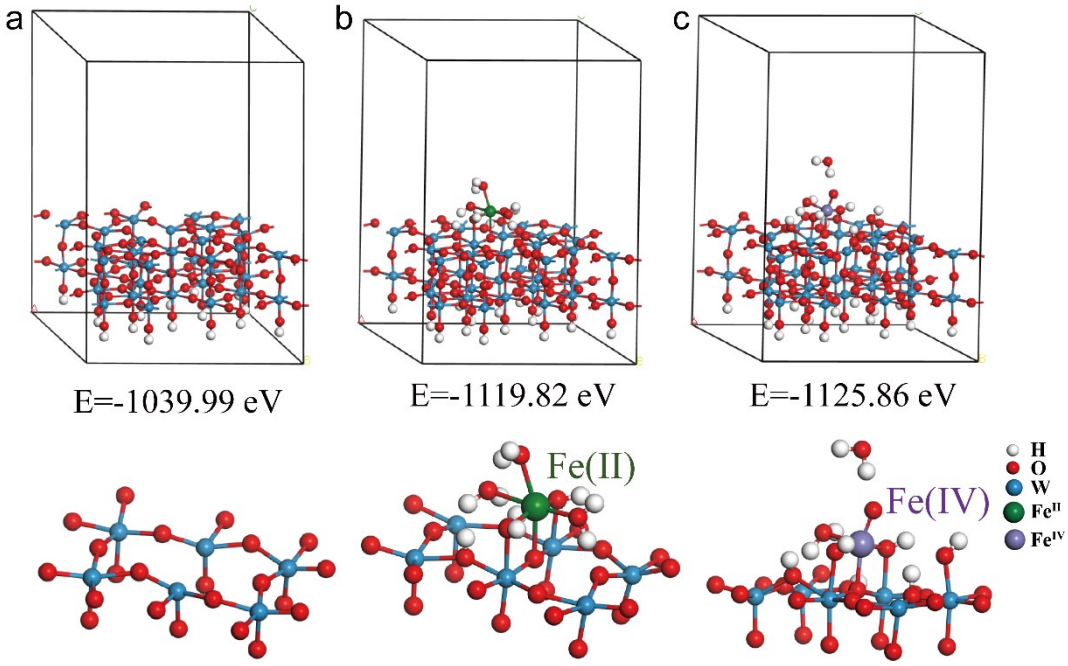

Figure S5 DFT-optimized models and energies. (a) Vo-containing {010} $WO_{2.72}$. (b) Fe^{II} and (c) Fe^{IV} complex on the Vo-modified surface.

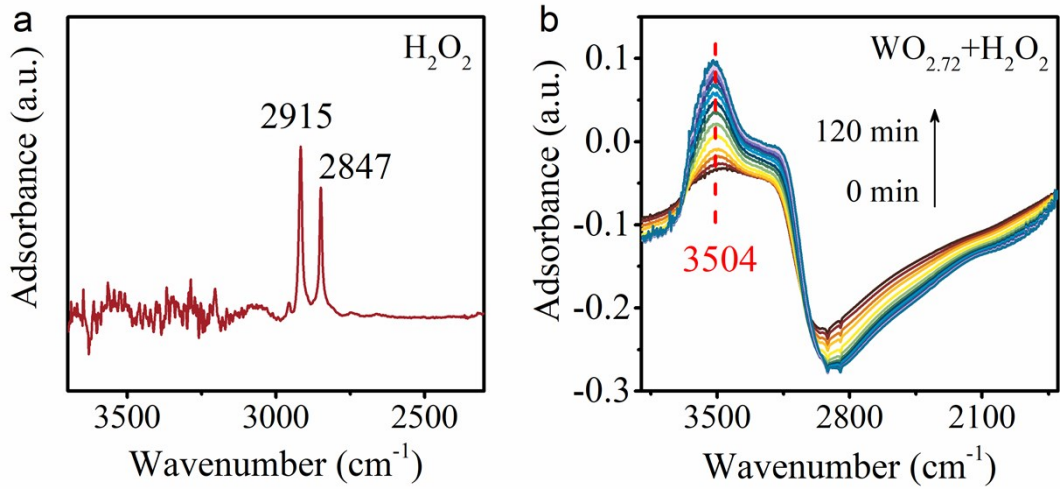

Figure S6 (a) FTIR spectra of H_2O_2 molecule. (b) *In-situ* flow cell FTIR spectra of H_2O_2 adsorption on the $WO_{2.72}$ surface.

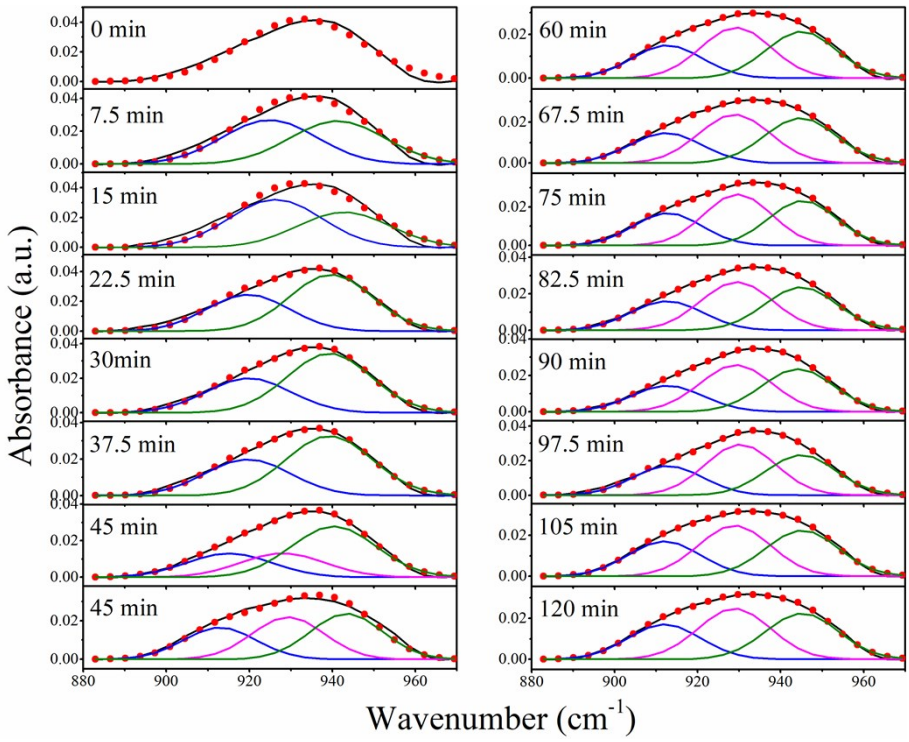

Figure S7 Observed (circles) and curve-fitting results (lines) of *in-situ* flow cell FTIR spectra of H_2O_2 reacted with bound- Fe^{II} on the $WO_{2.72}$ surface as a function of time.

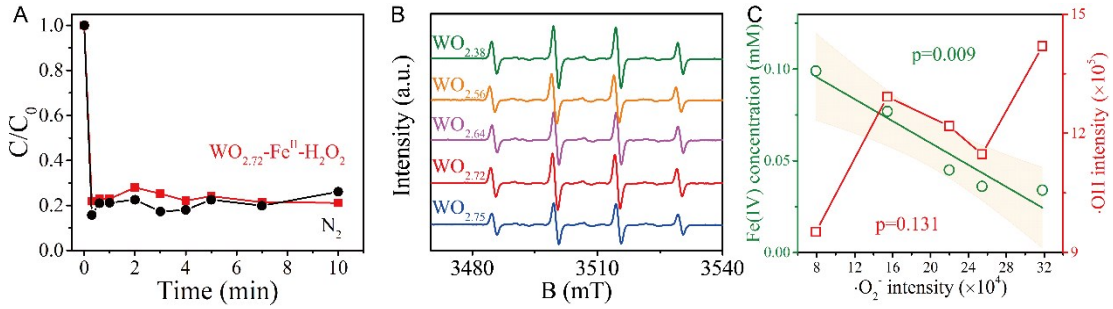

Figure S8 (a) MO removal in the Vo-dependent Fenton reaction with and without purging with N_2. (b) EPR spectra to detect ·OH in the Fe^{II}-H_2O_2-WO_{3-x} system. (c) Relationship between EPR intensity of DMPO-·O_2^- and DMPO-·OH (p=0.131), and linear dependence of EPR intensity of DMPO-·O_2^- on Fe^{IV} concentration (p=0.009).

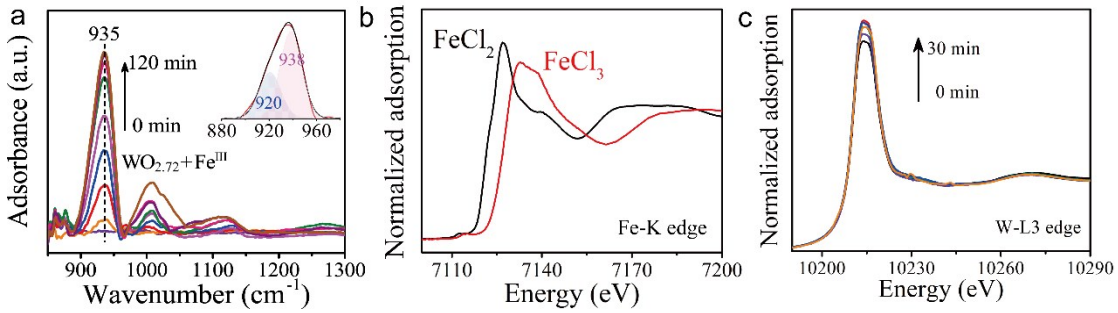

Figure S9 (a) *In-situ* flow cell FTIR spectra of Fe^{III} reacted with $WO_{2.72}$. (b) Fe K-edge XANES spectra of $FeCl_2$ and $FeCl_3$. (c) *In-situ* W L_3-edge XANES spectra of Fe^{III} reacted with $WO_{2.72}$ in the dark.

To explore the effect of surface-Vo on Fenton reactions, WO_{3-x} samples with different Vo densities were used as co-catalysts in degrading MO. As shown in **Fig. S10a**, the co-catalysts increased the MO degradation rate from 25% to 41-89%, approximately 1.6-3.5 times higher than that of the classical Fenton system. Notably, the degradation rate remained at ~90% after ten cycles with $WO_{2.38}$ (**Fig. S10b**), confirming the durability of Vo-enriched WO_{3-x}. In particular, the degradation rate was linearly correlated with the surface-Vo content (p=0.004, R^2=0.95, **Fig. S10c**) at the 95% confidence level, but not with the bulk-Vo (p=0.205). This correlation suggests that surface-Vo is central in heterogeneous Fenton catalytic reactions.

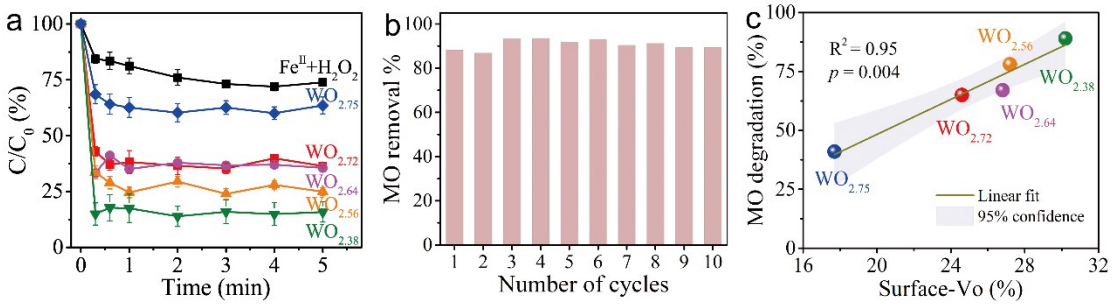

Figure S10 (a) Degradation of MO in the $WO_{2.75}$, $WO_{2.72}$, $WO_{2.64}$, $WO_{2.56}$, and $WO_{2.38}$ Fenton systems. (b) MO removal with $WO_{2.38}$ as co-catalysts after ten cycles. (c) A linear dependence of MO degradation rate on the surface-Vo percentage (p=0.004) at a 95% confidence level. The initial conditions: 50 mL of aqueous solution, 50 mg WO_{3-x}, 0.14 mmol/L Fe^{II}, 0.4 mmol/L H_2O_2, and 20 mg/L MO.

Table S1 Calculated electronic energies of the species. (All energy units are eV)

Species	E_{SP}
$\equiv OFe^{II}$	-1119.82
$\equiv OFe^{IV}O$	-1125.86
H_2O_2	-18.15
H_2O	-14.22

REFERENCES:

1. S. Cong, Y. Yuan, Z. Chen, J. Hou, M. Yang, Y. Su, Y. Zhang, L. Li, Q. Li, F. Geng and Z. Zhao, Noble metal-comparable SERS enhancement from semiconducting metal oxides by making oxygen vacancies, *Nat. Commun.*, 2015, **6**, 780.
2. J. P. Perdew, K. Burke and M. Ernzerhof, Generalized gradient approximation made simple, *Phys. Rev. Lett.*, 1996, **77**, 3865-3868.
3. L. Zhang, B. Wen, Y. Zhu, Z. Chai, X. Chen and M. Chen, First-principles calculations of water adsorption on perfect and defect WO_3(001), *Comp. Mater. Sci.*, 2018, **150**, 484-490.